# Thermal–electrical transport of high purity, melt impregnated, polycrystalline $MgB_2$



2011 Supercond. Sci. Technol. 24 085015

(http://iopscience.iop.org/0953-2048/24/8/085015)

Supercond. Sci. Technol. **24** (2011) 085015 (5pp) doi:10.1088/0953-2048/24/8/085015

# Thermal–electrical transport of high purity, melt impregnated, polycrystalline $MgB_2$

**E A Young, A Kulak and Y Yang**

School of Engineering Sciences, University of Southampton, SO17 1BJ, UK

Received 13 May 2011
Published 7 July 2011
Online at stacks.iop.org/SUST/24/085015

**Abstract**
In the polycrystalline superconductor $MgB_2$ the fraction of cross section that carries electrical current was previously shown to be obtained from the normal state electrical resistivity. The latest single crystal measurements show the thermal transport properties of $MgB_2$ to be dominated by electrical transport. For the first time we apply the electrical cross section to the thermal conductivity of three polycrystalline samples with different grain size and porosity. It is found that the results can be readily discussed in the context of granular thermal–electrical properties consisting of common temperature dependent transport properties independent of grain size and porosity. The result gives an alternative interpretation to the temperature dependent thermal transport than given in previous publications.

## 1. Introduction

Further fundamental materials research on $MgB_2$ bulk and wire conductors is still required to help successfully achieve potential applications from cables to magnetic resonance imaging (MRI) magnets. A case in point is the limited data on the thermal conductivity in polycrystalline (PC) and single crystal (SC) samples [1–5]. Thermal conductivity data are not only useful for thermal stability calculations for bulk conductors but in the understanding of the electronic properties that relate to pinning and critical current density. Data from SCs are generally accepted to be the most reliable measure of the intrinsic properties, but it is particularly difficult to measure thermal conductivity on small samples, (∼1 mm) more so than resistivity. On the other hand measurements of polycrystalline samples although easier to acquire are subject to intergrain effects, originating from surface scattering at grain boundaries, impurities and porosity. In this work we will explore whether the intergrain effects in polycrystalline samples can be accounted for to assess the possibility of extracting intrinsic properties from polycrystalline samples.

A model to account for intergrain effects has been applied to resistivity data [6, 7]. SC properties can be potentially extracted from PC measurements by scaling the temperature dependent resistivity with an effective cross section $F$. This method has been shown to be effective in accounting for porosity and oxide inclusions in samples where the $MgB_2$ grain boundaries are otherwise well connected [8], but the principle has so far not been used in the analysis of thermal conductivity.

The most recent measurement of thermal conductivity to date on SCs concludes that the heat is essentially conducted by electrons [1]. In this case the effective cross section should be the same for both thermal and electrical transport properties. In this paper we obtain the effective cross section, $F$, from the resistivity data and apply it to the thermal conductivity data. It is anticipated that if successful the method could prove to be useful to measure the intrinsic thermal conductivity and in extracting the level of impurity scattering from below $T_c$, in zero field, or above the critical field where the resistivity is not available.

## 2. Experimental details

To avoid complication by impurities, and percolation, high purity, well connected, PC samples were fabricated. The high quality samples were achieved by using the melt impregnation method [9]. 99.9% boron powder, $<1$ $\mu$m, was packed into a Ta (99.9%) lined Fe (98%) crucible, to 40% density, then a Mg rod (99.9%) was packed on top and a vacuum applied before the crucible was welded shut. The three samples were produced using different heat treatments. Sample 1, 750 °C for 10 h, sample 2 850 °C for 10 h, and sample 3 1000 °C for 1 h, 930 °C for 3 h, 800 °C for 10 h. The reacted pellets, turned out of the crucibles in a lathe, were initially very reactive

 

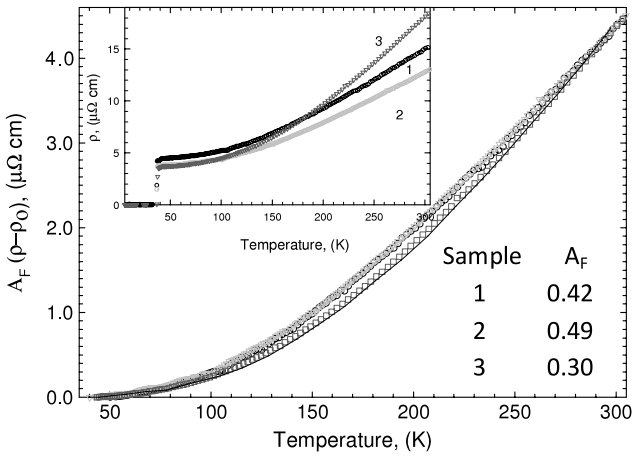


**Figure 1.** The reduced temperature dependent resistivities, $A_F(\rho - \rho_0)$, of samples 1 (black circles), 2 (light grey triangles) and 3 (grey squares), taken from the raw data, (inset), are compared. The reduced temperature dependent resistivity of sample 3, matches that of the single crystal (black line) the most closely. The values of $A_F$ used are included in the graph.

to air and water, yet no degradation within 1 year has been measured, showing the density to be sufficiently high to limit oxidation to the bulk surface. A surface layer of 0.5 mm was ground away to ensure no contamination from the Ta or Fe in the measured sample before 12 mm long bars were diamond cut to a square cross section of 0.5–1 mm$^2$. Electron microscopy was used to confirm that the microstructure viewed over 10 $\mu$m was consistent up to the sample length scale. For the contacts it was found that using only silver loaded epoxy did not produce the best joints. Instead pressure contacts for the electrical contact were made with custom made, hardened copper clip springs, with one side bonded with silver loaded epoxy for mechanical support and thermal contact. Resistivity and thermal conductivity were measured on the same section of sample in a Quantum Design PPMS. The largest error of 10% came from the finite size of the contacts.

## 3. Results and discussion

### *3.1. Resistivity*

The effective cross section, $A_F$, the factor proposed to remove artefacts of processing, such as porosity, which are irrelevant to understanding the electron flow, was obtained from the temperature dependent resistivity (inset figure 1). The residual resistivity was first subtracted and the temperature dependent part reduced by the factor $A_F$, until a close match to the temperature dependent curve of the single crystal values was obtained, (figure 1) [10]. The values of $A_F$ obtained were quite high compared to many polycrystalline samples in the literature, (<0.2), showing the high purity and high density of the samples [6–8]. It has been more common in the literature to simply divide the temperature dependent value numerically by the temperature dependent resistivity of the single crystal, which in figure 1 corresponds to a $\Delta\rho^{SC} = 4.3\ \mu\Omega$ cm. However, it has been pointed out that amounts of residual magnesium smaller than that detectable by techniques such as x-ray diffraction can significantly alter the effective cross section calculated in this way, and the presence of magnesium can be better observed as a smaller slope at higher temperatures [11]. For sample 3 the temperature dependence was a close match to the single crystal. Samples 2 and 3 were less satisfactory with a lower slope at high $T$ observable, and this is discussed later with the thermal conductivity and electron microscopy results. An attempt was made to fit the data by including the effect of a Mg parallel layer, but a satisfactory improvement was not obtained. The residual resistivity values obtained after this treatment are shown in table 1 to be discussed later together with the residual thermal resistance.

**Table 1.** The calculated intrinsic residual scattering properties taken from both electrical and thermal measurements and compared with the grain size.

| Sample (°C | Mean grain size ($\mu$m) | $\rho_0$ 40 K ($\mu\Omega$ cm) | $L_0\beta$, 40 K ($\mu\Omega$ cm) |
|---|---|---|---|
| 1, 750 | 0.55 | 1.89 | 1.57 |
| 2, 850 | 0.81 | 1.91 | 1.57 |
| 3, 950 | 1.37 | 1.08 | 0.93 |

### *3.2. Thermal conductivity*

The measured thermal conductivity for the three samples is shown in figure 2(a). The data are hard to reconcile with a picture of the same material but with different amounts of electron scattering. Although sample 3 has the most distinct peak at low temperatures, due to less scattering, it has a lower thermal conductivity at higher temperatures. What they do have in common is weak temperature dependence above 200 K. A temperature independent thermal conductivity would be expected at temperatures approaching the Debye temperature when the maximum phonon frequency is reached, due to no further increase in the phonon–electron scattering. Most published values of Debye temperature are from 600 to 900 K, however there is an analysis which separates the optical phonon modes (Einstein) from the acoustic (Debye) and consequently calculates a Debye temperature of around 400 K [12]. Although measurements to higher temperatures would be required to confirm that the temperature independent region is already reached at 350 K, it currently appears plausible to assume that this is the case for the purposes of this analysis.

Applying the effective cross section to the thermal conductivity, so plotting $k/A_F$ in figure 2(b), all three plots converge above 200 K to within the experimental error (10%). The overall picture, expecting values below $T_c$, is what would be measured in a fully dense metal with different amounts of electron scattering. Approaching the Debye temperature, the thermal conductivity values are the same, (within experimental resolution), and independent of electron scattering, because the residual effect reduces with increasing temperature as $1/T$. At lower temperatures sample 3, which has the most distinct peak, consistently has the highest thermal conductivity, and samples

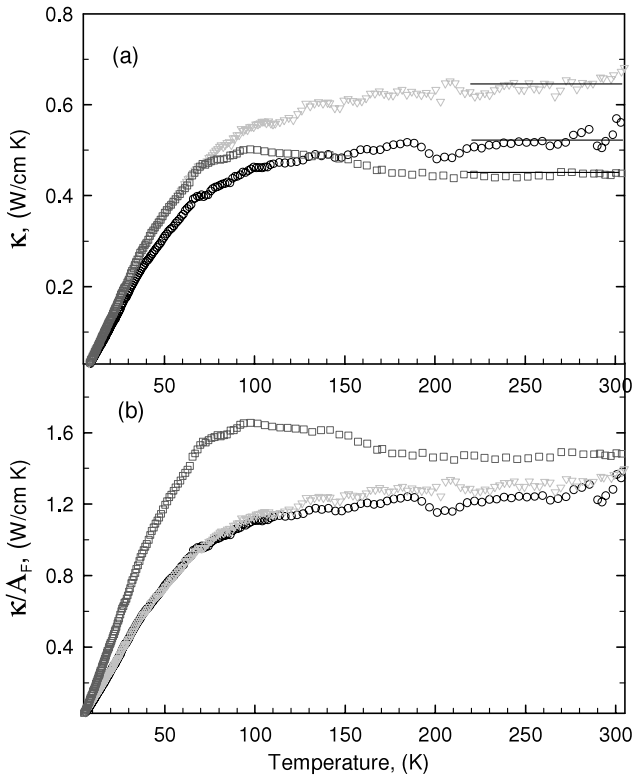


**Figure 2.** The thermal conductivity as measured, top (a), and divided by the effective cross sections $A_F$, bottom (b), from figure 1, for sample 1 (circles), sample 2 (light grey triangles) and sample 3 (grey squares). The solid three lines in (a) show the region, for $T > 200$ K where the temperature dependence is weak.

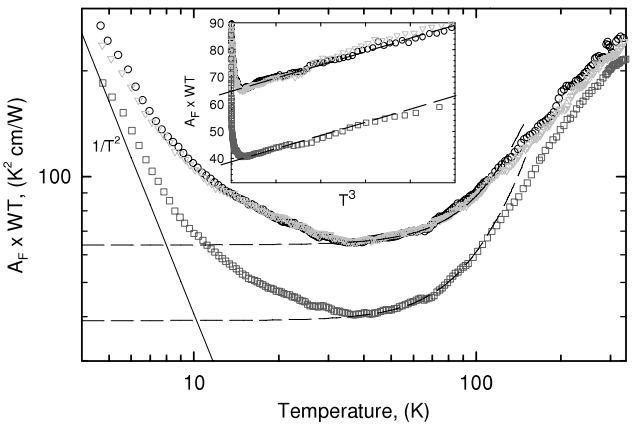


**Figure 3.** The effective thermal resistance $A_F W$, plotted as $A_F WT$, for sample 1 (circles), sample 2 (light grey triangles) and sample 3 (grey squares). The dashed line is $\beta + \alpha T^3$ with $\alpha =$ and $\beta =$ for the bottom curve (sample 3) and $\beta =$ (samples 1 and 2). Inset is $A_F WT$ plotted against $T^3$. The dashed lines show $\beta + \alpha T^3$ extended beyond the axis with the same value of $\alpha$.

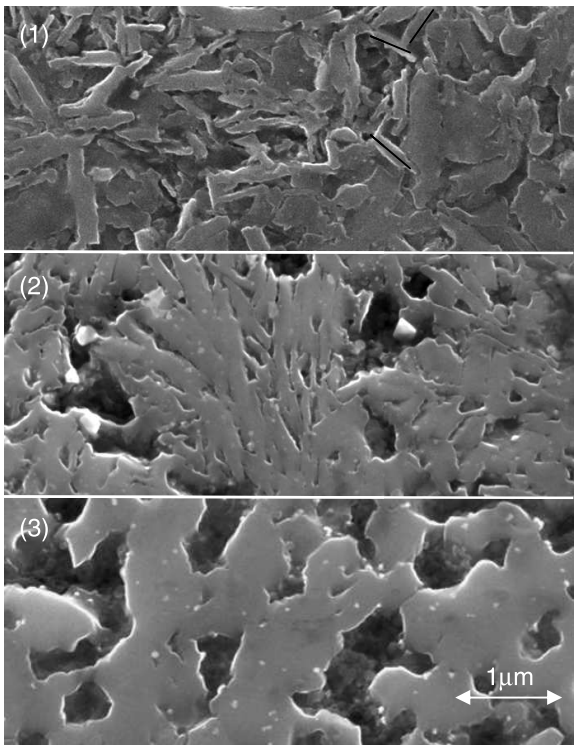


**Figure 4.** From top to bottom, secondary electron microscope images of samples 1, 2 and 3.

1 and 2 are almost identical with an overall lower thermal conductivity.

At temperatures well below the Debye temperature, about $\theta/10$, the thermal resistance ($W = 1/k$) depends on temperature for an electronic conduction of heat as, $W = \beta/T + \alpha T^2$. The first term, $\beta$ is the residual thermal resistance and the second term $\alpha$ relates to the electron–phonon scattering. The concept of electrical resistivity is generally more familiar, so it can be easier to visualize the residual scattering when plotted as $WT = \beta + \alpha T^3$, as for electronic conduction of heat $\rho \propto WT$ where the proportionality constant is the Lorenz number. Again using the effective area, $A_F WT$ is plotted in figure 3. The residual resistance is seen as the minimum at 40 K, though this is not conclusive as there is plainly a change of slope below $T_c$, and without this effect it may decrease further (which is also true in the resistivity). With increasing temperature $A_F WT$ increases as $T^3$ (dashed line), until about 100 K where it naturally deviates from this behaviour because $T \gg \theta/10$. The same value of $\alpha = 2.4 \pm 0.2 \times 10^{-7}$ cm W$^{-1}$ K$^{-1}$ was used to plot the dashed lines, and no significant difference in the fundamental phonon scattering is observed despite the wide range in porosity and grain size of the samples (seen in figure 4).

With decreasing temperature from 40 K the resistance also increases, in a quite clear deviation from that expected for electronic conduction of heat, as seen by the dashed line. The increased thermal resistance below $T_c$ is evidently due to the reduced number of electrons transporting heat, as in other superconducting materials where electrons are the main carriers. The decrease in heat transport by the electrons with temperature may be increasingly replaced by phonon heat conduction, but this does not appear to be rapid, as by 6 K, there is not yet a $1/T^2$ boundary scattering dependence (figure 3, straight line). The latest single crystal measurements in fact show the electronic conduction of heat to be dominant down to 2 K [1].

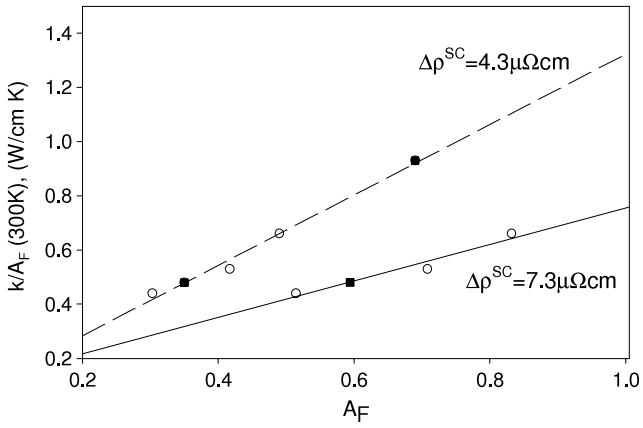


**Figure 5.** The intrinsic thermal conductivity ($k/A_F$) at 300 K calculated using a $\Delta\rho$ (300–40 K) of 4.3 $\mu\Omega$ cm (dotted line top) and 7.3 $\mu\Omega$ cm (solid line bottom). Open circles are samples from this paper. Filled squares are calculated from data for samples in [3].

As discussed in the resistivity measurements, it is possible that some residual magnesium in samples 1 and 2 is affecting the temperature dependence, but on viewing the thermal resistance values it is unlikely to be significant. The thermal conductivity of 99.9% pure magnesium increases up to 15 W cm$^{-1}$ K$^{-1}$ at 20 K, about 150 times higher than the measured values, so more likely to affect the thermal conductivity than the resistivity, then decreases rapidly. If even 1% of magnesium was affecting the thermal conductivity values it would be seen at 20 K, and unique to samples 2 and 3. Electron microscopy images, figure 4, show some small localized bright spots, most likely Mg, or MgO, (too small to identify by energy dispersive spectroscopy), but much less than 1%, and not forming a continuous conduction path.

Table 1 shows the values obtained for $L_0\beta$ and $\rho_0$ after applying the effective cross section, using a Lorenz number of $2.45 \times 10^{-7}$. The values for $L_0\beta$ are proportionate to the $\rho_0$ values, but about 15% smaller. This could be interpreted as a larger Lorenz number being required, or that the dimensional distance between the contacts is not identical for thermal and electrical measurement. Better spatial resolution would be achievable if longer samples with a consistent microstructure could be synthesized, which would better answer this question.

The microstructure of the samples is seen in figure 4 to have increasing grain size with increasing synthesis temperature, (table 1). At this time it looks as though there is no direct link between grain size and residual resistance, as sample 2, although having identical residual resistance to sample 1, clearly has a larger average grain size (table 1). This result is not inconsistent with the expected scattering mean free path of the electrons which is estimated to be around 240 Å for 1 $\mu\Omega$ cm residual resistivity near $T_c$ [10], and so independent of the grain size. This would also imply that the scattering is instead dependent on the annealing of defects in the grain during synthesis.

### *3.3. Reference sample*

More than one SC reference sample has been used in the literature for the value of $\Delta\rho$ to calculate $A_F$, the smallest value is 4.3 $\mu\Omega$ cm and the largest 7.3 $\mu\Omega$ cm, yet with no consensus [6, 7]. To explore the effect of using a different reference value on the results, the application of the effective cross section to the thermal conductivity was performed with both these values. Further to this, data from high purity samples from the literature were also included [3]. The temperature dependent resistivities of the PC samples from [3], were found to be a close match to the single crystal. Furthermore, the 300 K thermal conductivity results were the same within 10%. The 300 K thermal conductivity values are plotted in figure 5 against the effective cross section for both the 4.3 and 7.3 $\mu\Omega$ cm cases. In this way the plots can be extrapolated to a $k$(300 K) value for a theoretical 100% dense sample and this value used as an alternative reference value to $\Delta\rho$. For the lower line representing the 7.3 $\mu\Omega$ cm value, the as-measured 300 K values for one of the PC Puti samples were found to be higher than the extrapolated 100% dense value. This also correlates to the $\Delta\rho$ for this sample being smaller than 7.3 $\mu\Omega$ cm. Using $\Delta\rho^{SC} = 4.3$ $\mu\Omega$ cm, all the PC samples have a value less than that for 100% dense and show a linear extrapolation to a 100% dense value of ~1.3 W cm$^{-1}$ K$^{-1}$. Although such a high value of the single crystal thermal conductivity at 300 K remains to be verified, with a reliable value of the single crystal thermal conductivity at room temperature, the effective cross section can be calculated from the room temperature thermal conductivity, independently of the resistivity. This has the distinct advantage of not requiring any cryogenics for the measurement. It may also be useful as an independent measurement of the fundamental properties especially when more complicated samples with impurities and percolation are considered.

## 4. Conclusions

After applying the effective cross section $A_F$ the thermal conductivities of all three samples can be described independently of inter-granular effects. Care was taken to examine the possibility of residual magnesium affecting the data and no evidence of any residual material was found. The approach of a temperature independent thermal conductivity above 200 K is consistent in all samples and reduces as $A_F$ $k$ (300 K) to a common value. The use of the effective cross section gives an alternative explanation to the temperature dependent behaviour of high purity samples than another theoretical framework put forward to date [3]. Furthermore, no percolation models were required in order to explain the temperature dependent thermal transport, likely due to the high density and lack of oxides at grain boundaries. A single value of electron–phonon scattering, $\alpha = 2.4 \pm 0.2 \times 10^{-7}$ cm W$^{-1}$ K$^{-1}$ satisfactorily describes all the samples yet the thermal residual is independent and consistent with the resistivity residual. The Lorenz constant was found to be about 15% larger than the theoretical value, though measurements on longer samples with better spatial resolution and at higher temperatures (>300 K) would better resolve this. Using this method with data from the high purity samples in this publication and from the literature the value for thermal conductivity at 300 K was extrapolated as 1.3 W cm$^{-1}$ K$^{-1}$.

## References


[1] Sologubenko A V, Zhigadlo N D, Karpinski J and Ott H R 2006 *Phys. Rev.* B **74** 184523
[2] Pope A L *et al* 2003 *J. Appl. Phys.* **93** 5531–7
[3] Putti M, Braccini V, Galleani E, Napoli F, Pallecchi I, Siri A S, Manfrinetti P and Palenzona A 2003 *Supercond. Sci. Technol.* **16** 188–92
[4] Schneider M *et al* 2001 *Physica* C **363** 6–12
[5] Cavallin T, Young E A, Beduz C, Yang Y and Giunchi G 2007 *IEEE Trans. Appl. Supercond.* **17** 2770–3
[6] Rowell J M 2003 *Supercond. Sci. Technol.* **16** R17–27
[7] Jiang J, Senkowicz B J, Larbalestier D C and Hellstrom E E 2006 *Supercond. Sci. Technol.* **19** L33–6
[8] Eisterer M, Emhofer J, Sorta S, Zehetmayer M and Weber H W 2009 *Supercond. Sci. Technol.* **22** 034016
[9] Giunchi G *et al* 2005 *IEEE Trans. Appl. Supercond.* **15** 3230–3
[10] Eltsev Yu, Lee S, Nakao K, Chikumoto N, Tajima S, Koshizuka N and Murakami M 2002 *Phys. Rev.* B **65** 140501(R)
[11] Jung C U *et al* 2002 *Physica* C **377** 21–5
[12] Masui T, Yoshida K, Lee S, Yamamoto A and Tajima S 2002 *Phys. Rev.* B **65** 214513